CHAPTER 4

RESULTS AND DISCUSSION OF RESULTS

The experimental results of this study are presented as follows :

4.1 The adsorption isotherms.

The adsorption isotherm for the system of n-hexane-cyclohexane over coconut shell based activated carbon at 15 °C expressed in term of surface excess is presented in figure 4.1.

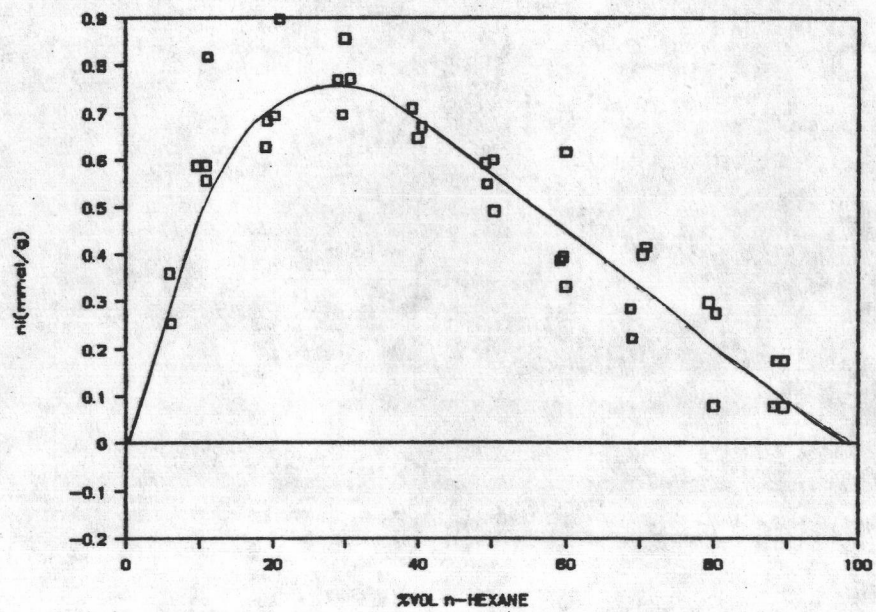

Figure 4.1 The excess of n-hexane in a mixture of n-hexane and cyclohexane on activated carbon at 15 °C.

Isotherms may also be presented in terms of a Freundlich equation in the form

$$q = b C^{\beta} \qquad (4.1)$$

where q is amount of solute adsorbed in mg/ml adsorbent and C is the concentration of solute in the liquid mixture in mg/ml.

However it is to be noted that q is the actual moles of solute adsorbed and not a surface excess . But q may be obtained from surface excess data by incorporating the lotal pore volume inside the adsorbent using measurements as shown in appendix E. The data for q as a function of C is shown in appendix B.

The data is presented in terms of ln(q) as a function of ln(C) in figure 4.2. This plot is used to calculate constants b and β in the Freundlich eqaution . For the Freundlich isotherm in terms of n-hexane the values of b and β have been measured at b = 4.379 and β = 0.7447. The Freundlich equation is now shown in comparison with experimented data in figure 4.3. The same can be done for cyclohexane as shown in 4.4 with the values of b and β being b = 0.41 and β = 1.097. Both sets of data are of course valid for temperatures of 15°C ($\pm$ 1°C). It is of course possible to relate contration of n-hexane in binary mixture to volume percent of n-hexane by dividing by the specific gravity of n-hexane at 15 °C (0.662) and to relate contration of cyclohexane in the binary mixture to volume percent of cyclohexane by dividing by the specific gravity of cyclohexane at 15°C (0.779).

The representation of isotherms following a Freundlich equation is convenient for the calculation of breakthrough curves.

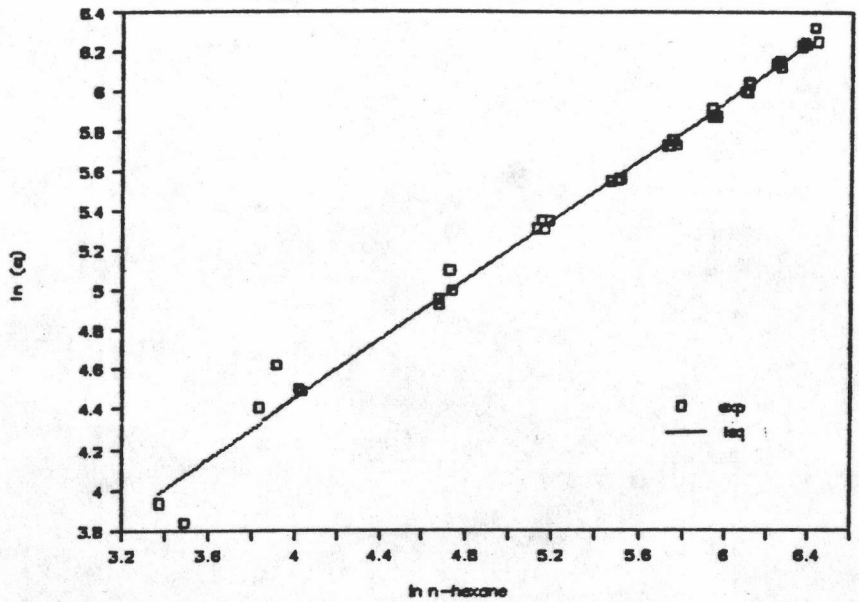

Figure 4.2 Plot ln(q) vs ln C of n-hexane in mixture of n-hexane and cyclohexane on extivated carbon at 15 °C.

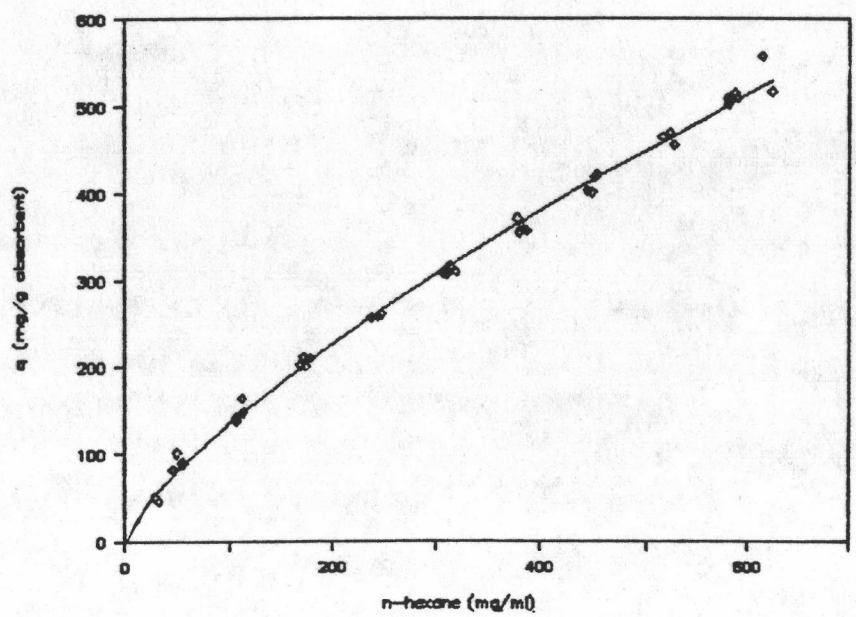

Figure 4.3 The adsorption isotherm of n-hexane in mixture of n-hexane and cyclohexane on activated carbon at 15°C.

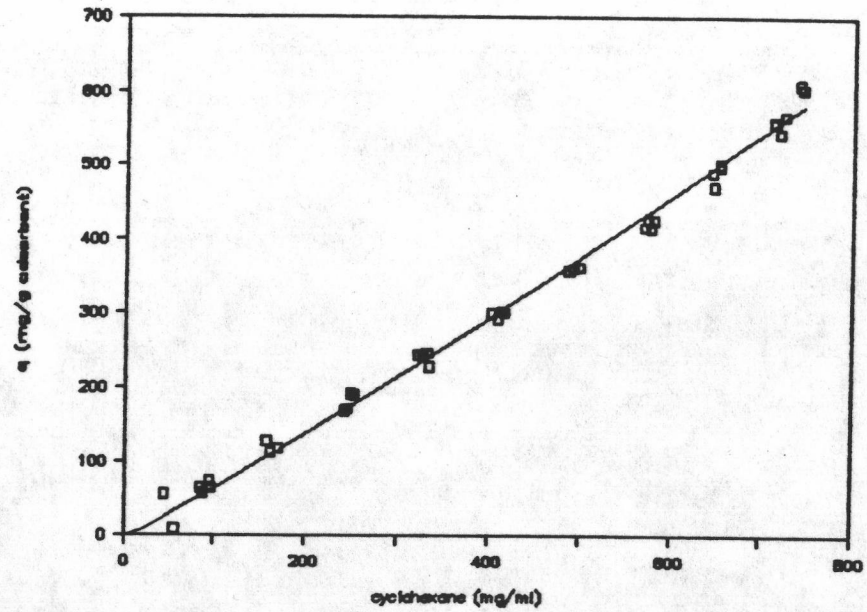

Figure 4.4 Adsorption isotherm of cyclohexane in mixture of n-hexane and cyclohexane on activated carbon at 15 C.

4.2 The adsorption constants.

During the derivations of the basic equations describing adsorption in a column, a number of hypotheses were made. The first hypothesis is the existence of a film outside the adsorbent pellet and hence the existence of a film mass transfer coefficient k_f (cm/min). This coefficient was not measured in this study as it was felt that it could be obtained from published correlations going back several years. The second hypothesis was the existence of axial dispersion flow in the liquid phase leading to an axial dispersion coefficient D_l (cm^2/min) and here again this coefficient was not measured in this study as it was felt that it could be obtained from known correlations widely recognized. The

third hypothesis was the transport of solute inside the pellets for which a number of models were available and in this study it was decided that intraparticle coefficient would be surface diffusion model leading to a surface diffusion coefficients D_s (cm^2/min). In this study D_s was measured experimentally through batch experiments as the literature had no data available for the system of interest in this study. The fourth hypothesis was that the combination of external resistance and internal resistance led to an overall mass transfer coefficient K_c (cm/min) that could be used in the design equation of the adsorption column.

The values of the above mentoned parameters are presented as follows.

4.2.1 The axial dispersion coefficients

The axial dispersion coefficients in packed beds were calculated using equation E.5 of appendix E (5). Sample calculations are shown in appendix E , and the entire set of calculation results which correspond to experimental data conditions are presented in table V.

Table V

Calculated axial dispersion coefficients

	Co(mg/ml)	Uo(cm/min)	Z(cm)	D_1 (cm^2/min)
1	150.27	1.59	46.00	0.6775
2	238.32	1.53	44.50	0.6482
3	332.98	2.90	46.50	1.1165
4	157.35	2.94	45.50	1.1618
5	140.34	3.70	47.00	1.4191
6	139.21	2.40	48.00	0.9761

4.2.2 The external mass transfer coefficients the surface diffusion coefficients and the overall mass transfer coefficients.

The external mass transfer coefficient is obtained from equation E.7 in appendix E(5). The intraparticle diffusion coefficient also referred to as surface diffusion coefficient was obtained from experimental data presented in appendix D based on a methology presented by K.Hashimoto and K. Mirura (5). The overall mass transfer coeffient was calculated from equation E.11 in appendix E (4) using both external mass transfer coeffient and surface diffusion coefficient . All three coeffient are tabulated in table VI .

The values of the coefficients may be injected in the equation to obtain breakthrough curves (as shown in appendix E).

All six breakthrough curves are presented in figures 4.5 to 4.4.10 and compared with the experimental data . It is to be noted that the data fit the model reasonably well except at large times.

Table VI

The calculated external mass transfer coefficients (k_c), surface diffusion coefficients form the experimental system (D_s), and the calculated overall mass transfer coefficient (Kc).

	Co mg/ml	Ds X 10^{6} cm^2/min	kf X 10^{2} cm/min	Kc X 10^{5} cm/min
1	150.27	1.0640	3.0871	9.6425
2	238.32	1.0640	3.3289	9.6447
3	332.98	1.0640	5.4661	9.6556
4	157.35	1.0640	4.4557	9.6517
5	140.34	1.0640	5.0072	9.6540
6	139.21	1.0640	3.8788	9.6486

In order to try to remedy this discrepancy it was decided to makes use of the experimental breakthrough curves to obtain the external mass transfer coefficient through the numerical optimization process while keeping the surface diffusion coefficient constant. The results are tablulated in table VII and presented in figure 4.11 to 4.16 and compare with the experiment data. The new values of the external mass transfer coefficients are different from the values obtained from correlation found in the

literature but the breakthrough curves are now closer to the experimental breakthrough curves. It is to be noted that the surface diffusion coefficient remains constant at 1.064×10^{-6} cm^2/min based on batch experimental data.

Table VII

The external mass transfer coefficient obtained through optimization of the breakthrough curves.

	Co mg/ml	Ds X 10^6 cm^2/min	kf X 10^2 cm/min	Kc X 10^5 cm/min
1	150.27	1.0640	0.7010	8.5000
2	238.32	1.0640	0.0877	4.6000
3	332.98	1.0640	0.0877	4.6000
4	157.35	1.0640	8.9200	9.5600
5	140.34	1.0640	0.1800	6.3000
6	139.21	1.0640	0.2050	6.5800

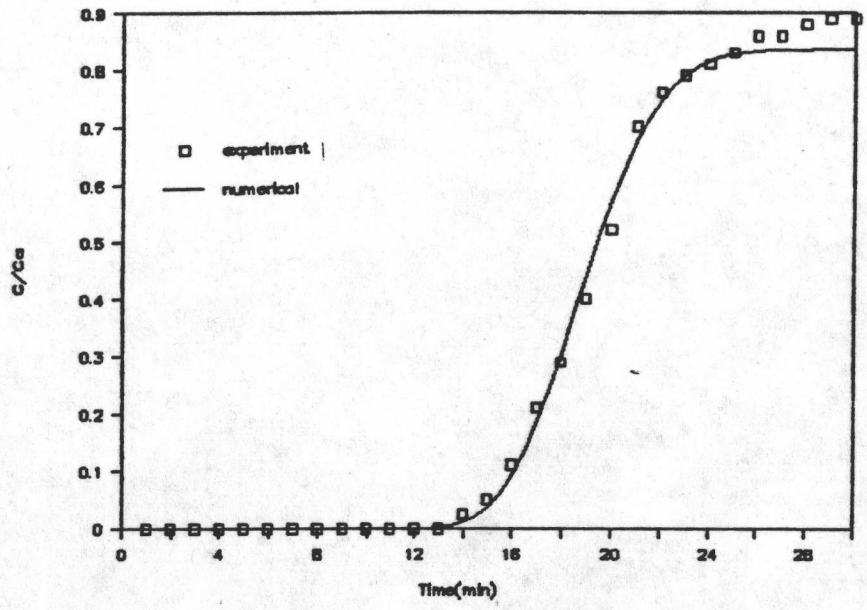

Figure 4.5 Breakthough curve for n-hexane ; Co 150.27 mg/ml Uo 1.59 cm/min and bed length 46.00 cm.

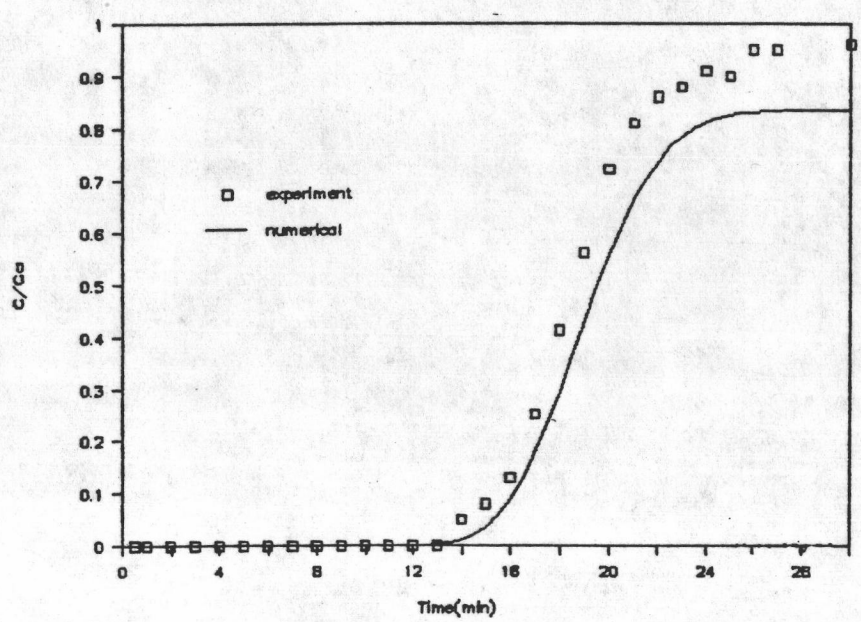

Figure 4.6 Breakthough curve for n-hexane ; Co 238.32 mg/ml Uo 1.53 cm/min and bed length 44.50 cm.

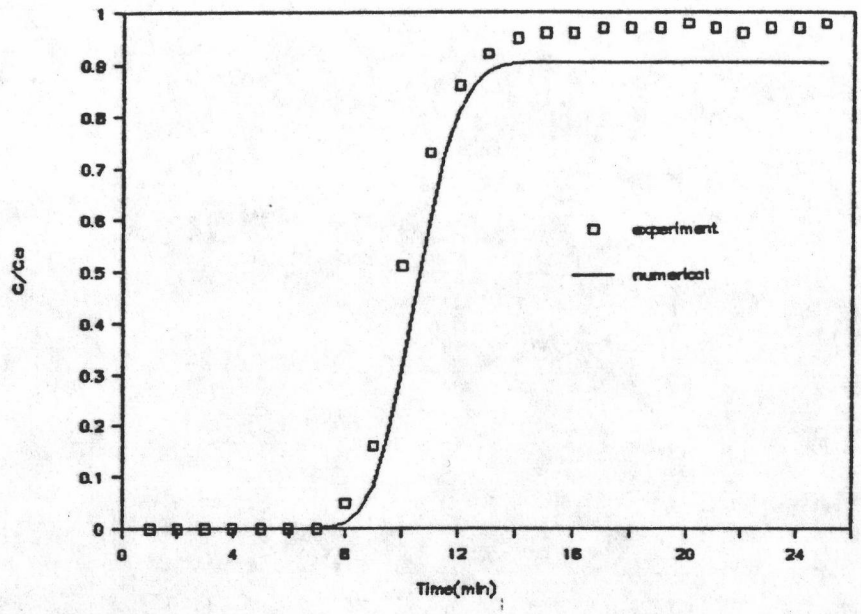

Figure 4.7 Breakthough curve for n-hexane ; Co 332.98 mg/ml Uo 2.90 cm/min and bed length 46.50 cm.

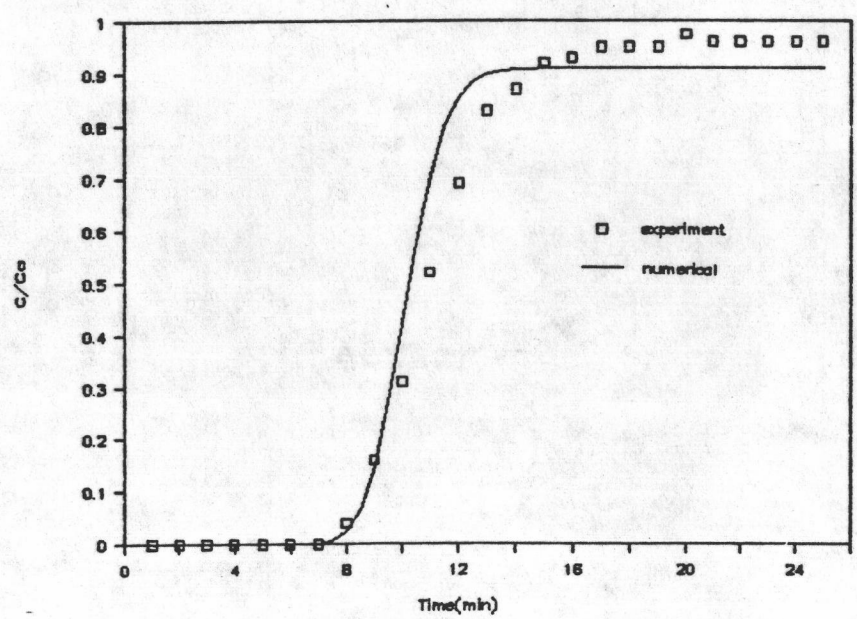

Figure 4.8 Breakthough curve for n-hexane ; Co 157.35 mg/ml Uo 2.94 cm/min and bed length 45.50 cm.

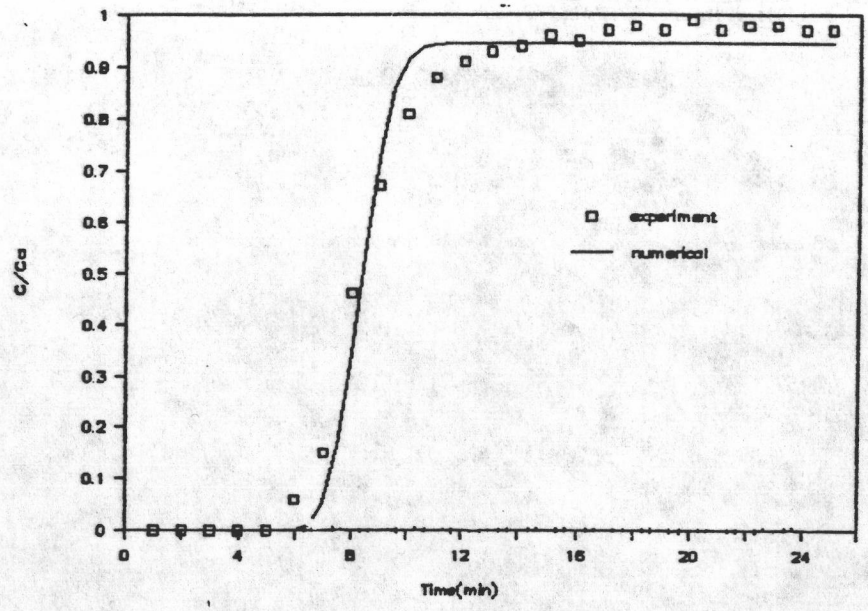

Figure 4.9 Breakthough curve for n-hexane ; Co 140.34 mg/ml Uo 3.70 cm/min and bed length 47.00 cm.

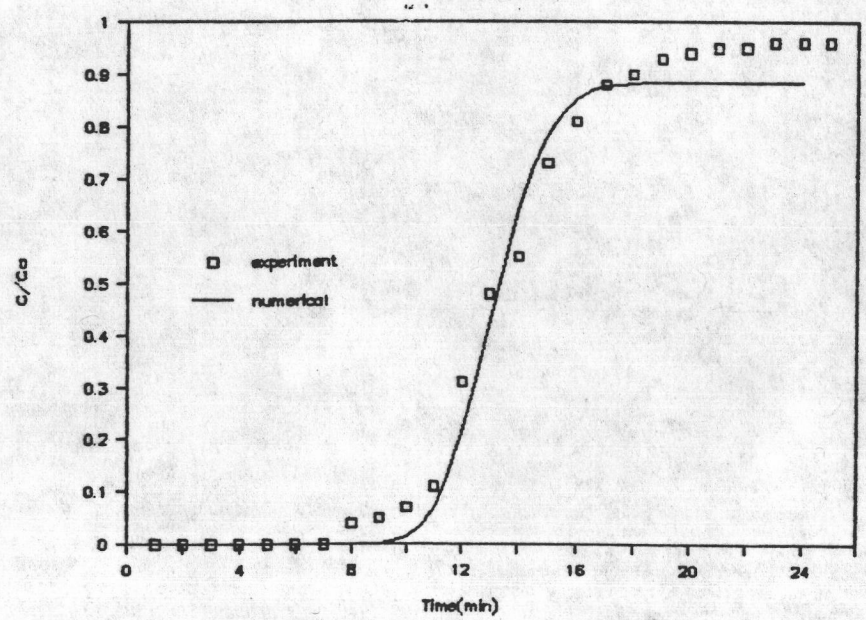

Figure 4.10 Breakthough curve for n-hexane ; Co 139.21 mg/ml Uo 2.40 cm/min and bed length.48.00 cm.

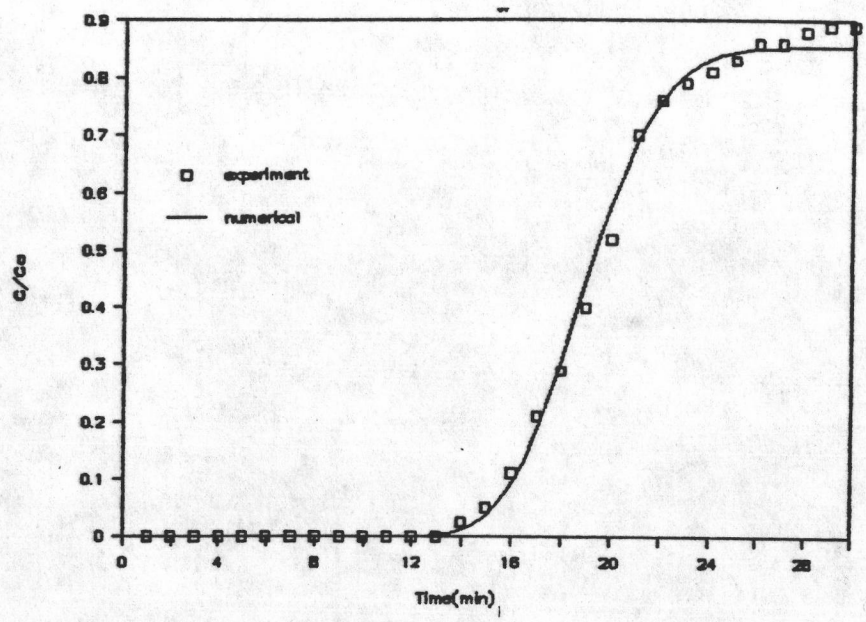

Figure 4.11 Breakthough curve for n-hexane ; Co 150.27 mg/ml Uo 1.59 cm/min and bed length 46.00 cm.

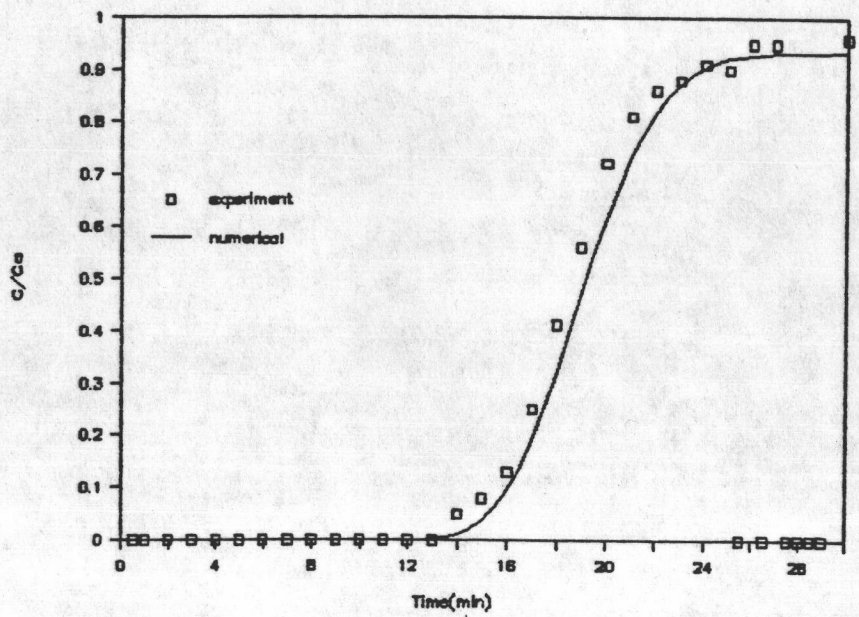

Figure 4.12 Breakthough curve for n-hexane ; Co 238.32 mg/ml Uo 1.53 cm/min and bed length 44.50 cm.

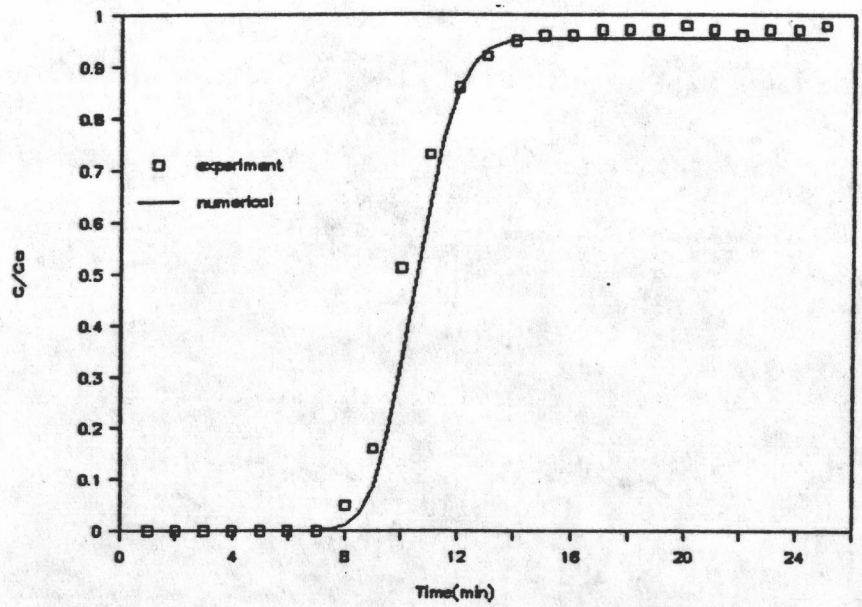

Figure 4.13 Breakthough curve for n-hexane ; Co 332.98 mg/ml Uo 2.90 cm/min and bed length 46.50 cm.

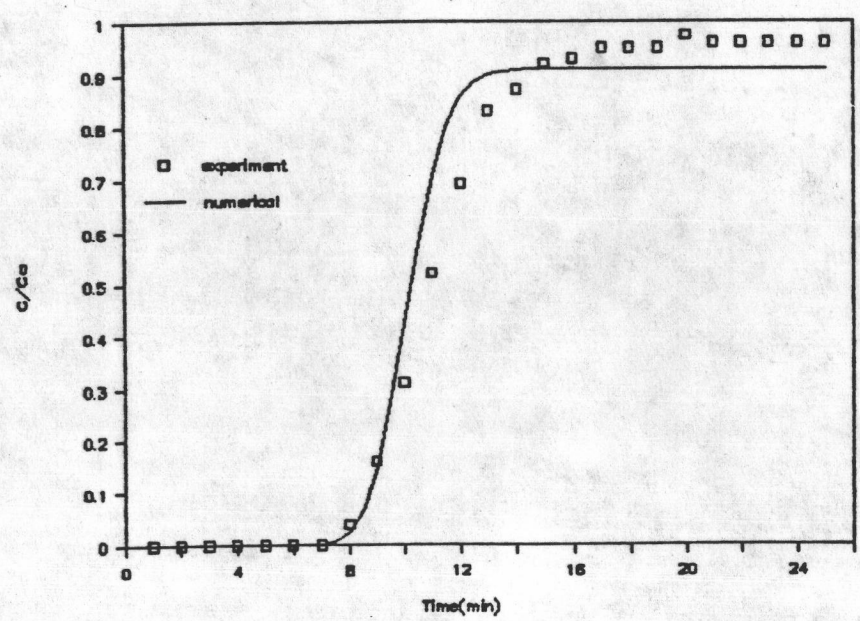

Figure 4.14 Breakthough curve for n-hexane ; Co 157.35 mg/ml Uo 2.94 cm/min and bed length 45.50 cm.

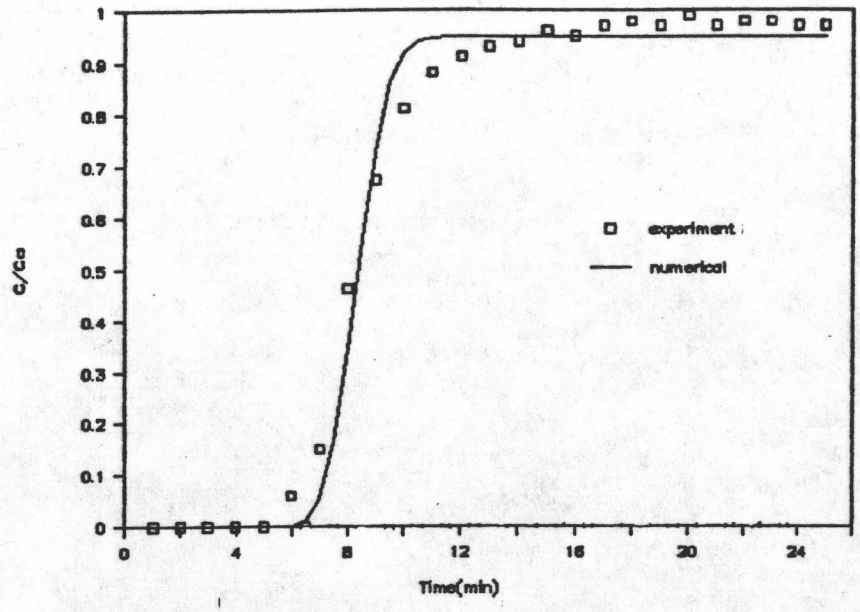

Figure 4.15 Breakthough curve for n-hexane ; Co 140.34 mg/ml Uo 3.70 cm/min and bed length 47.00 cm.

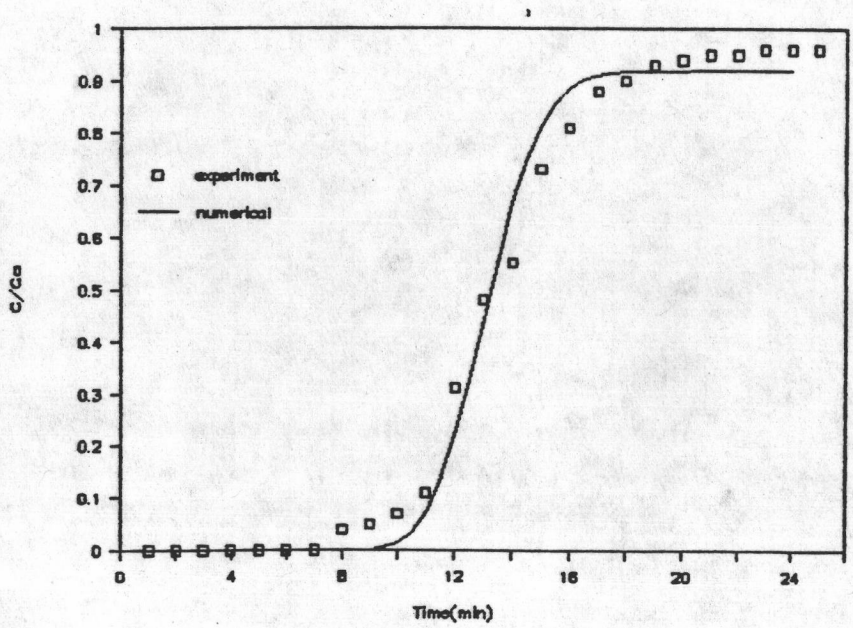

Figure 4.16 Breakthough curve for n-hexane ; Co 139.21 mg/ml Uo 2.40 cm/min and bed length 48.00 cm.

4.3 Disussions

4.3.1 The adsorption isotherms.

from figures 4.3 and 4.4 it is not obvious that n-hexane is more strongly adsorbed onto the activated carbon chose in this study over cyclohexane. However using the isotherm equations obtained one can draw an equilibrium diagram shown in figure 4.17 and based on calculation as shown in table VIII which indicates clearly that n-hexane is more strongly adsorbed over cyclohexane. A probable reason is that the n-hexane molecule is linear rather than disk like such as the case of cyclohexane and linear molecules ought to penetrate pores more easily.

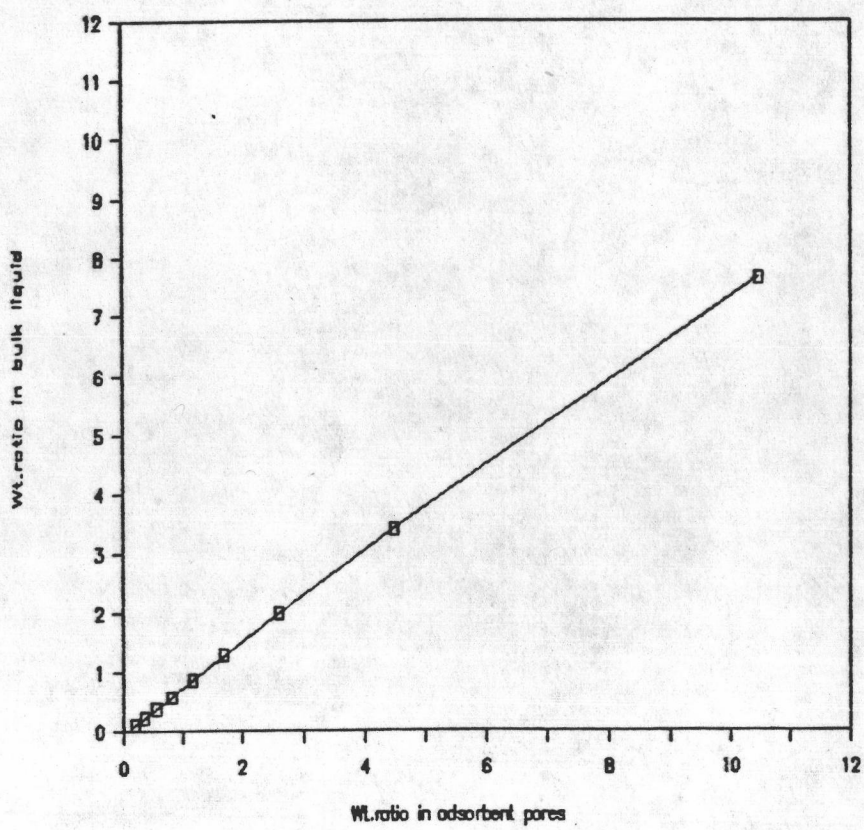

Figure 4.17 Equilibrium diagram for adsorption of a n-hexane-cyclohexane mixture on coconut shell based activated carbon.

Table VIII

Computation of equilibrium diagram

Weight ratio of n-hexane/cyclohexane	
adsorbent	bulk liquid
10.4759	7.6482
4.4860	3.3992
2.6032	1.9828
1.6927	1.2747
1.1569	0.8498
0.8022	0.5665
0.5467	0.3642
0.3491	0.2124
0.1831	0.0944

4.3.2 The intrapraticle diffusion coefficients.

The diffusion of solute inside the adsorbent pellet has been assumed to be a surface diffusion phenomena similarly to the assumption of most other researchers dealing with adsorption. Thus the intraparticle diffusion coefficient refers also to surface diffusion coefficient or D_s. D_s was obtained through unsteady-state batch experiments and a single value of 1.0640×10^{-6} cm^2/min was recorded. This value seems to lie within the range of intraparticles coefficients of between 1×10^{-5} and 1×10^{-6} cm^2/min

reported by D.M.Ruthven (9) for similar systems. Generally it is considered that intraparticle diffusion is the rate determining step , meaning that it is the slowest in particular when compared to the external or film mass transfer . During the calculation of the overall mass transfer coefficient which takes into account transfer through both zones , we may compare both resistances $(1/k_f)$ and $(D_p/10D_m)$ which add up to (1/Kc) and we realized that the external resistance is only 1/10 or 1/5 of the internal resistance this is a conclusion which agrees with the general case.

4.3.3 The external mass transfer coefficient

The external mass transfer coefficient as computed from published correlations did not yield the best breakthrough curves and in particular the concentrations were erroneous at long times. It was thus decided to optimize external mass transfer coefficients based on breakthrough curves and based on such optimized coefficients the agreement between breakthrough curve data and model was excellent. However the external mass transfer coefficients obtained by optimization were found to be much lower than the coefficients obtained through published correlations. Using the optimized coefficients the fit at high values of time was also very good. It is to be noted however that such optimization was made assuming the existence of reliable data on axial dispersion coefficients. The question of axial dispersion coeffients will be look at in the following section.

4.3.4 The axial dispersion coefficient

Data for axial dispersion coefficient in packed columns is very exhaustive and generally fairly reliable. This is the reason it was decided to use a published correlation (5) to compute D_l.

In an attempt to look at breakthrough curves without considering axial dispersion a comparison is presented in figure 4.18 which indicate that axial dispersion plays a very important role in determining the shape of the breakthrough curve.

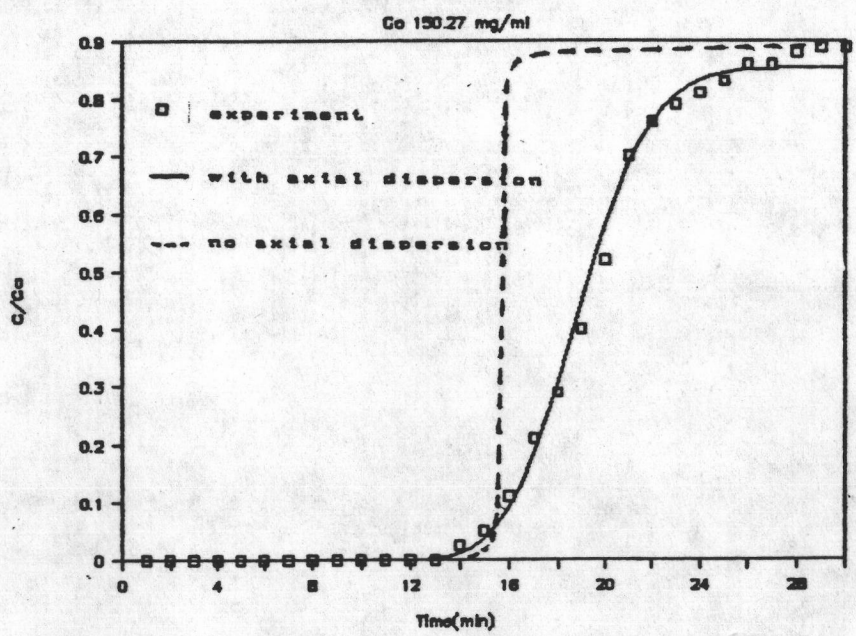

Figure 4.18 The effect of axial dispersion coefficient in the prediction of breakthrough curves.